

RESEARCH OF VIBRATION LEVELS IN SPECIFIC PARTS OF VEHICLE TRAVELING AT VARYING SPEED ON ROAD WITH DIFFERENT TYPES OF SURFACE

Deniss Brodnevs, Maris Hauka, Muharbi Banovs, Guntis Strautmanis,
Leonids Vinogradovs, Igors Scukins

Riga Technical University, Latvia

deniss.brodnevs@rtu.lv, maris.hauka@rtu.lv, mukharbiy.banov@rtu.lv,
guntis.strautmanis@rtu.lv, vile2@inbox.lv

Abstract. Development of measures to reduce the value of vibration velocity and vibration acceleration, arising on various elements of the car, allows to develop vehicles with high ergonomic indicators. Excitation of vibrations, first of all, is connected with different values of irregularities of a road surface, with mechanical parameters of the moving car (weight, rigidity of a suspension etc.), and also with speed of the car. Measurement equipment and vibration sensors during full-scale studies were placed in the car, and in order to reduce the error of the measurement results, the car speed was stabilized before passing the road section, on which the vibration was recorded. As the measuring and recording equipment were used: MMF sensor type KD45, signal amplifier Conditioning Amplifier B&K type 2626 and recording equipment USB Oscilloscope TiePie type HandyScope HS3. The vibration sensor was attached with a magnet in the luggage compartment of the car near the rear shock strut. The paper contains photos of the road surface, on which the measurements of vibration acceleration and vibration were done, as well as the results of processing the parameters of full-scale measurements of vibration.

Keywords: mathematical analysis, vibration, paved road, gravel cover road, asphalt road.

Introduction

Movement of a vehicle on a road, regardless of the surface type, unavoidably induces vibrations of (and within) all construction elements of the vehicle. Control over vibration level and research of methods and constructions capable to decrease vibration frequency and vibration amplitude in a vehicle would help in creating a vehicle with not only high ergonomics, but also long exploitation time, as vibration induced construction fatigue could be decreased using the same methods. Induced vibration is largely caused by the unevenness of the traversed roads, but it is also caused by mechanical properties of the vehicle itself (mass, toughness of the suspension, (miss-) alignment of rotary elements in engine, transmission, wheels etc.), travel speed also has strong effect on induced vibrations.

This paper covers results of the experiments, where the vibration was measured in the cargo compartment of a passenger car, as well as the created mathematical model of the vehicle and road, describing the same process. Measurements were made at various discreet movement speeds ranging from $10 \text{ km}\cdot\text{h}^{-1}$ to $60 \text{ km}\cdot\text{h}^{-1}$ on three types of road surface- stone paving, gravel road and asphalt. Asphalt cover also got separate measurements at $80 \text{ km}\cdot\text{h}^{-1}$.

The paper also examines the calculation method and mathematical model of the vehicle movement. The mathematical model considers the vehicle as a set of masses. Each of the mechanism's elements connected with tough joints is considered as one mass (elements fixed together with bolts, rivets, welded etc.), and then these fixed masses connected to others through flexible joints (such as shock absorbers, springs, rubber tires etc.) Only the most prominent directions of the vibration caused by traversing the road are considered for the mathematical model and experiments.

This paper is a continuation of a whole series of previous experiments and research.

The goal of this paper is to experimentally determine the vibration level in a specific location of a vehicle (cargo is of the vehicle where sensitive and highly precise vacuum equipment would be placed in perspective) depending on the movement speed ($10\text{-}80 \text{ km}\cdot\text{h}^{-1}$) on roads with different cover type.

Gathering of vibration level data

When a vehicle is moving along a road, the surface irregularities and crevices are transmitted to all parts of the vehicle, both internal and external, in the form of shock pulses [1; 2], this also makes it more difficult to analyse the measurement results. In addition, the amplitude of the road surface irregularities and their length are random, effectively reducing any acquired measurement results to a mere collection of random variables only useable as average level indication [3]. The paper considers a method that would simplify the problems to the road modelling caused by road irregularities, a mathematical method

that would make it possible to set up a test stand and through it the set up, repeat or adjust the road conditions that would accurately correspond to the road properties.

During the previous stage of the research, it was determined, that the largest amplitude of vibrations happens in the vertical (Z) axis, while vibrations in the sideways direction (X and Y axis respectively) have significantly smaller amplitude than the aforementioned Z axis. Due to this reason, it was decided to record only the vertical component of the vibrations.

During the research, data was gathered while commencing travel on a passenger car on public roads with various covers:

- cobblestone paving – a public road in a city, covered with processed stone (see Fig. 1);
- gravel road – a gravel road in a city, well maintained with no pits, potholes or ruts (see Fig. 2);
- asphalt cover – a fresh asphalt highway outside of a city with no signs of wear yet (see Fig. 3).

The road surface types used for the studies, were selected based on the studies of other previous research and authors [4; 5], however, a comparative analysis on the vibration levels induced in the cargo compartment by various road surfaces has not been researched before [6].



Fig. 1. Cobblestone paving in city made of processed stone. Well maintained



Fig. 2. Gravel cover road in a city. Well maintained, without potholes



Fig. 3. Asphalt highway outside of a city with no signs of wear

Vibration level measurements were made at the following fixed speed settings within $10 \text{ km}\cdot\text{h}^{-1}$ to $80 \text{ km}\cdot\text{h}^{-1}$ speed bracket: $10 \text{ km}\cdot\text{h}^{-1}$; $20 \text{ km}\cdot\text{h}^{-1}$; $30 \text{ km}\cdot\text{h}^{-1}$; $40 \text{ km}\cdot\text{h}^{-1}$; $50 \text{ km}\cdot\text{h}^{-1}$; $60 \text{ km}\cdot\text{h}^{-1}$. Additionally, vibration levels on the asphalt cover were taken at $80 \text{ km}\cdot\text{h}^{-1}$ as well.

To minimize the measurement error, the speed of the vehicle was stabilized for at least 15 seconds before the measurements were taken.

The following measuring and data recording devices were used: Sensors MMF type KD45; signal amplifier Conditioning Amplifier B&K type 2626; For recording of data USB Oscilloscope TiePie type HandyScope HS3 was used.

Vibration sensor was fixed in place of measurement using magnetic locks. The exact place of the vibration sensor placement was in the cargo compartment of the car near the right-side shock absorber.

The parameters of the amplifier and recorder oscillograph were set to match the ones used during the previous series of research for more comprehensive cross-reference of data at later time.

Table 1

Measuring and data recording device parameters

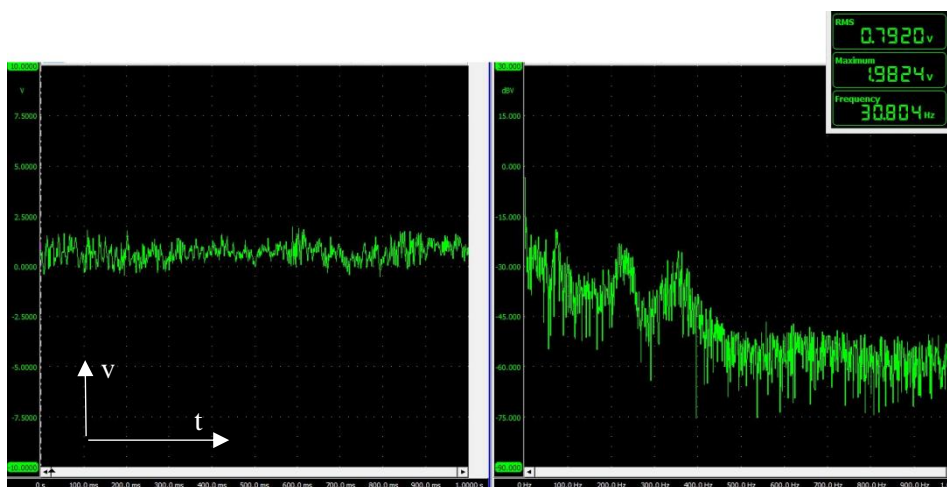
Amplifier	
LPF	1 kHz (-3 dB)
HPF	Direct (0.3 Hz at -3 dB level), floating point
Attenuator	10 V/G
Oscillograph	
Discretisation frequency	2 kHz
Resolution of ADC	14 bits
Network	DC
Memory length	2 KS

Gathered vibration level data

The experimentally acquired vibration level data from sensors are processed and stored in detail. It includes data in form of rms (root mean square) and peak values of vibro-acceleration, spectrograms, as well as sorted in the table.

Fig. 4 to Fig 9 show rms and peak values of vibroacceleration taken by the sensor while driving on a paved road at speed $10 \text{ km}\cdot\text{h}^{-1}$ to $60 \text{ km}\cdot\text{h}^{-1}$.

Comparing Fig. 4-6, it can be deduced that the travel speed has a significant effect on the vibration level in the cargo compartment of the vehicle; the vibration level increases the faster the vehicle travels over paved road.

Fig. 4. $10 \text{ km}\cdot\text{h}^{-1}$ on paved road

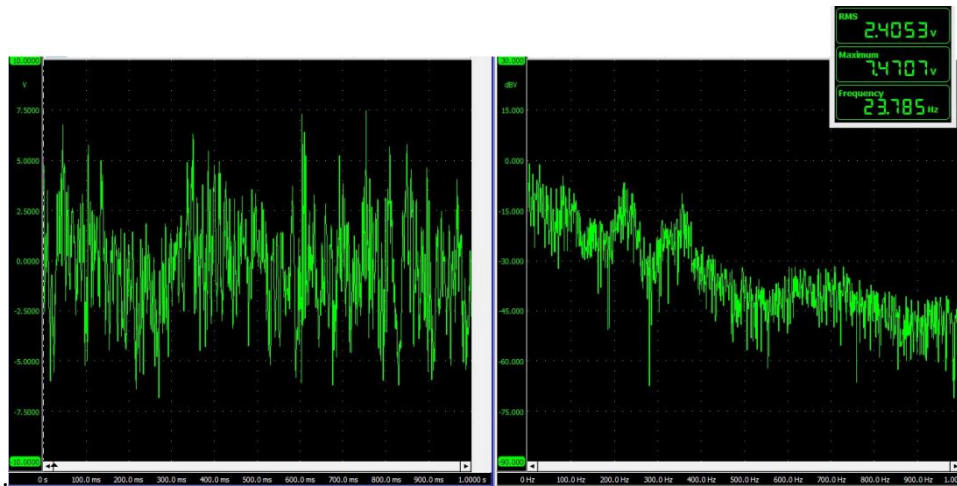


Fig. 5. 40 km·h⁻¹ on paved road

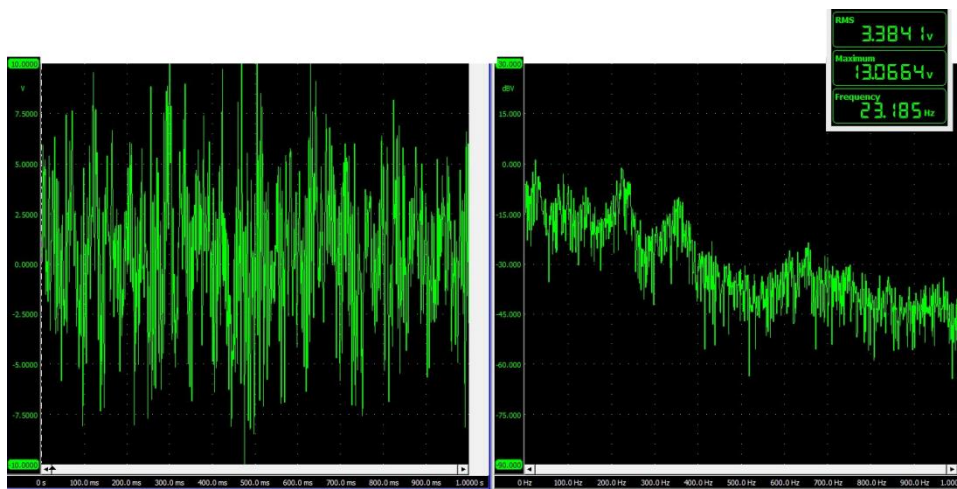


Fig. 6. 60 km·h⁻¹ on paved road

Fig. 7-8 show rms and peak values of vibroacceleration taken by the sensor while driving on a gravel road at speed 10 km·h⁻¹ to 60 km·h⁻¹.

Comparing Fig. 7-9, it can be deduced that the travel speed still has a significant effect on the vibration level in the cargo compartment of the vehicle on the gravel road as well.

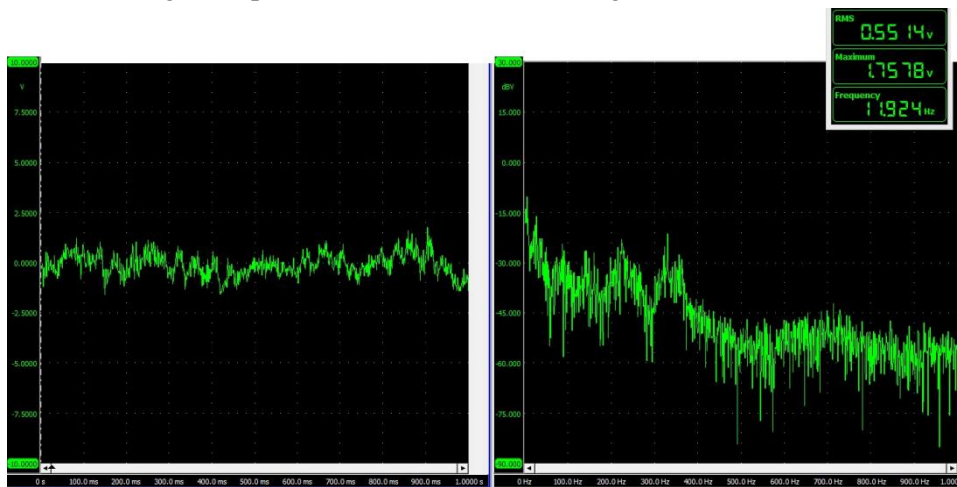


Fig. 7. RMS and peak values while traveling with 10 km·h⁻¹ on gravel road

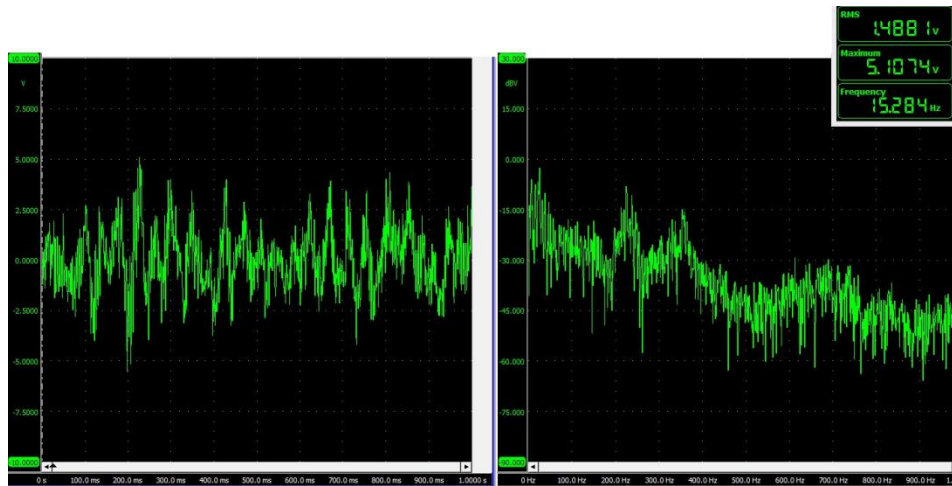


Fig. 8. RMS and peak values while traveling with 40 km·h⁻¹ on gravel road

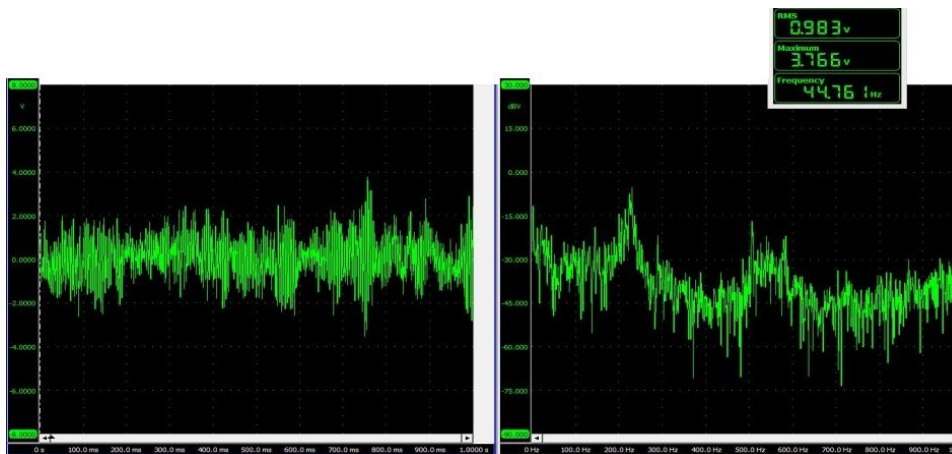


Fig. 9. RMS and peak values while traveling with 80 km·h⁻¹ on asphalt road

When comparing the data corresponding to the image groups Fig. 4-6 and Fig. 7-9, it can be concluded that the general trend of the vibration level increasing with the increase of the travel speed holds true for both paved and gravel road. As expected, the vibration level at each step is higher when traveling on paved road, whereas gravel road shows comparatively a lot lower vibration levels in each corresponding step. Measurements on asphalt further proved the fact. As a result, graphs of only the highest travel speed on asphalt are directly shown. The measurement data was processed using the methodology shown in [7].

Processed vibration level data

Vibration data has been summarized in Tables 2-5.

Table 2

Vibration values on stationary vehicle chassis and idling engine

Speed, km·h ⁻¹	Acceleration rms, m·s ⁻²	Acceleration peak, m·s ⁻²	Mean frequency, Hz
0	0.024	0.057	33.4

Table 3

Vibration values on vehicle moving on asphalt cover road

Speed, km·h ⁻¹	Acceleration rms, m·s ⁻²	Acceleration peak, m·s ⁻²	Mean frequency, Hz
80	0.098	0.38	44.7

Table 4

Vibration values on vehicle moving on gravel cover road

Speed, km·h ⁻¹	Acceleration rms, m·s ⁻²	Acceleration peak, m·s ⁻²	Mean frequency, Hz
10	0.055	0.18	11.9
20	0.069	0.22	13.2
30	0.13	0.24	17.8
40	0.15	0.51	15.3
50	0.21	1.01	10.7
60	0.25	1.02	14.6

Table 5

Vibration values on vehicle moving on paved cobblestone cover road

Speed, km·h ⁻¹	Acceleration rms, m·s ⁻²	Acceleration peak, m·s ⁻²	Mean frequency, Hz
10	0.093	0.34	7.15
20	0.14	0.5	14.1
30	0.24	0.75	23.8
40	0.28	0.99	19.6
50	0.34	1.31	23.2
60	0.44	1.15	33.4

The graphs below show the same vibroacceleration RMS, peak and average values, but this time shown together for ease of comparison. All graphs show the values of all three road cover types at the measured speed points.

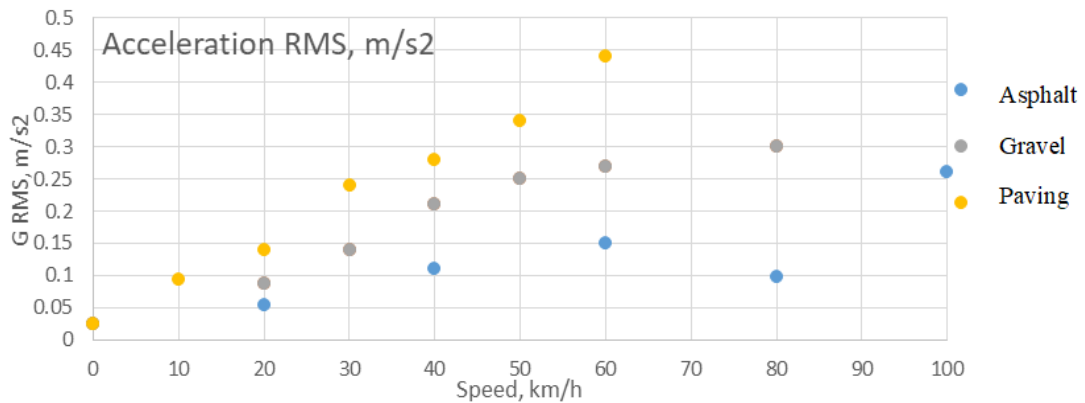


Fig. 10. Vibroacceleration rms values at various speed values on all three types of road covers

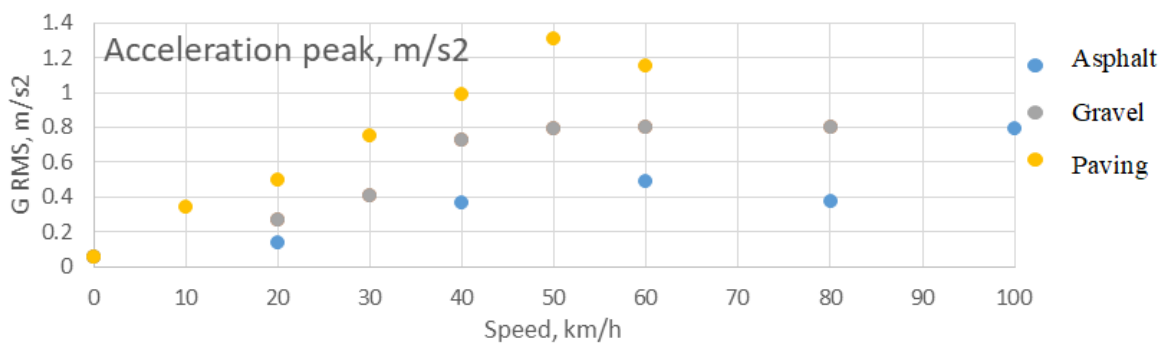


Fig. 11. Vibroacceleration peak values at various speed values on all three types of road covers

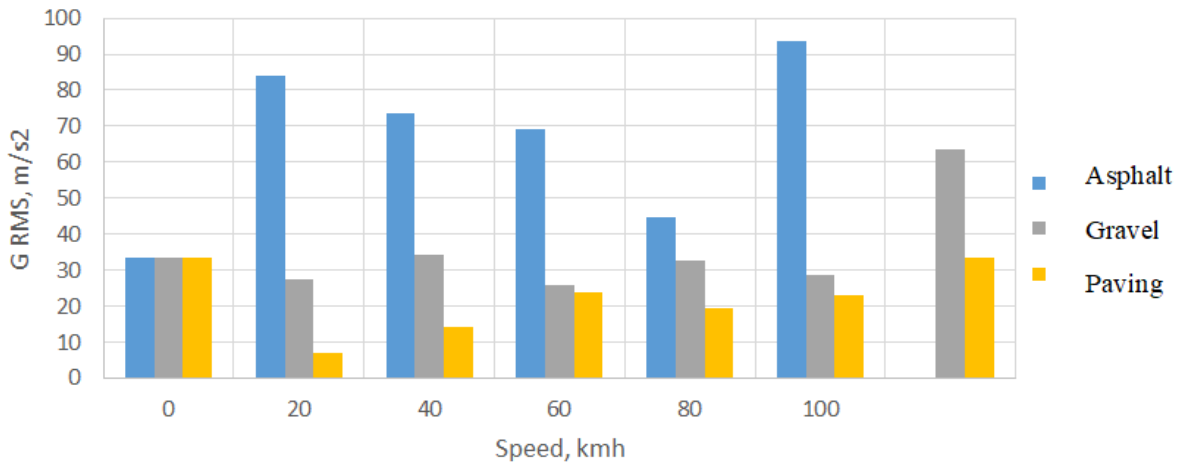


Fig. 12. Vibroacceleration average values at various speed values on all three types of road covers

Mathematical model of the vehicle

The vehicle for mathematical modelling purposes can be represented as an oscillating system comprised of separate hard masses- the chassis, the wheels, the engine, the cargo compartment etc. Though some of these are fixed to each other via hard, inflexible joints, they can still be divided in groups connected through flexible joints and dampener systems. The calculating method is based on the values shown in Fig. 13 [8].

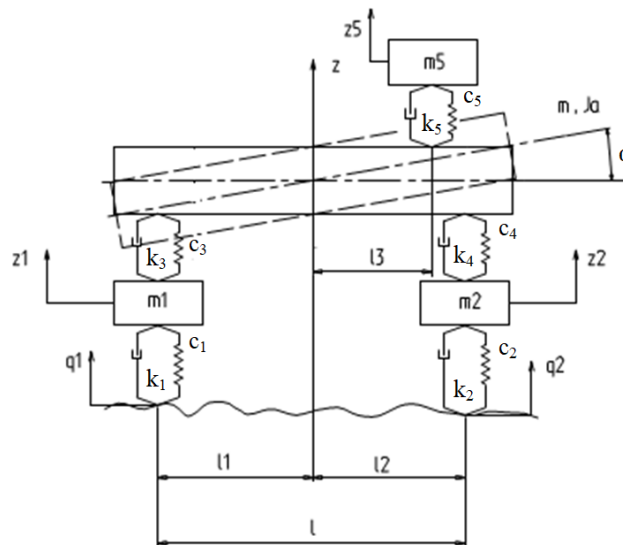


Fig. 13. Mathematical model of the vehicle

The hard bodies are initially divided in spring-loaded bodies (or masses) and not spring-loaded bodies (or masses). As spring-loaded are considered all the elements, the mass of which is passed to/through flexible suspension elements and joints. Not spring-loaded elements are considered those, the mass of which is not passed to such flexible suspension elements and joints, but through only fixed joints. As spring-loaded in a car would be considered the chassis and the cargo compartment as well as the elements affixed onto them, among such would also be the “cargo” (in perspective- the vacuum device described in the annotation) anchored to the cargo compartment in the rear of the car (mass m_5). Not spring-loaded would be the wheels and their assembly with the axles.

The goal of the mathematic calculations of the vehicle model is to determine the parameters of the flexible connections linked to the cargo compartment of the vehicle, so as to better describe the actual

situation in the cargo hold. This would in long run allow to better describe possible vibration levels in the required part of vehicle without need for direct practical experiment. And through this knowledge-how to minimize the vibrations in a vehicle transferred from the road to the body of the vehicle. As explained previously, the sensor was fixed in the cargo compartment of the car, fixed magnetically to the suspension's right shock absorber and can be considered as depicting the situation of what the cargo would have experienced.

In order to research the vertical vibration component of a vehicle, the mathematical model is made to consist of four masses that are considered to be able to oscillate in four modes.

To describe the behaviour of the mathematical model a second order differential equation is used derived from Lagrange equation of second order **Error! Reference source not found.** Equations of oscillation (movement) **Error! Reference source not found.** are made for the following conditions:

- Chassis and wheels are oscillating mildly;
- Characteristics of all elements (except the shock absorbers) are linear;
- Axis of all masses considered in the model match the main ellipsoid axis of the inertia;
- Only vertical forces are considered to be affecting the vehicle while the horizontal plane is aligned with the centre of the mass of the chassis.

$$m_1 \cdot \ddot{z}_1 + c_1 \cdot (z_1 - q_1) - c_3 \cdot (z - l_1 \cdot \alpha - z_1) + k_1 \cdot (\dot{z}_1 - \dot{q}_1) - k_3 \cdot (\dot{z} - l_1 \cdot \dot{\alpha} - \dot{z}_1) = 0, (1)$$

$$m_2 \cdot \ddot{z}_2 + c_2 \cdot (z_2 - q_2) - c_4 \cdot (z + l_2 \cdot \alpha - z_2) + k_2 \cdot (\dot{z}_2 - \dot{q}_2) - k_4 \cdot (\dot{z} + l_2 \cdot \dot{\alpha} - \dot{z}_2) = 0, (2)$$

$$m \cdot \ddot{z} + c_3 \cdot (z - l_1 \cdot \alpha - z_1) + c_4 \cdot (z + l_2 \cdot \alpha - z_2) - c_5 \cdot (z_5 + l_3 \cdot \alpha - z) + k_3 \cdot (\dot{z} - l_1 \cdot \dot{\alpha} - \dot{z}_1) + k_4 \cdot (\dot{z} + l_2 \cdot \dot{\alpha} - \dot{z}_2) - k_5 \cdot (\dot{z}_5 + l_3 \cdot \dot{\alpha} - \dot{z}) = 0, (3)$$

$$I_a \cdot \ddot{\alpha} - c_3 \cdot l_1 \cdot (z - l_1 \cdot \alpha - z_1) + c_4 \cdot l_2 \cdot (z + l_2 \cdot \alpha - z_2) + c_5 \cdot l_3 \cdot (z_5 + l_3 \cdot \alpha - z) - k_3 \cdot l_1 \cdot (\dot{z} - l_1 \cdot \dot{\alpha} - \dot{z}_1) + k_4 \cdot l_2 \cdot (\dot{z} + l_2 \cdot \dot{\alpha} - \dot{z}_2) + k_5 \cdot l_3 \cdot (\dot{z}_5 + l_3 \cdot \dot{\alpha} - \dot{z}) = 0, (4)$$

$$m_5 \cdot \ddot{z}_5 + c_5 \cdot (z_5 - z + l_3 \cdot \alpha) + k_5 \cdot (\dot{z}_5 - \dot{z} + l_3 \cdot \dot{\alpha}) = 0, (5)$$

where m_1 – not spring-loaded mass of the front axle of the vehicle;
 m_2 – not spring-loaded mass of the rear axle of the vehicle;
 m – spring-loaded mass of the vehicle (including m_5 in the cargo compartment);
 I_a – moment of inertia of spring-loaded mass relative to the transverse axis of the vehicle passing through the centre of its masses;
 m_5 – mass of the cargo in the luggage compartment;
 c_1 and k_1 – hardness and coefficient of deformation of the front tires;
 c_2 and k_2 – hardness and coefficient of deformation of the rear tires;
 c_3 and k_3 – hardness and coefficient of deformation of the front suspension;
 c_4 and k_4 – hardness and coefficient of deformation of the rear suspension;
 $l = 2760$ mm – vehicle base;
 $l_1 = 1380$ mm – distance from the centre of the masses to the front axle;
 $l_2 = 1380$ mm – distance from the centre of the masses to the rear axle;
 $l_3 = 1000$ mm – distance from the centre of the masses to the cargo fixation point;
 z_1 – vertical movement of the not spring-loaded mass of the front axle of the vehicle.;
 z_2 – vertical movement of the not spring-loaded mass of the rear axle of the vehicle;
 z – vertical movement of the not spring-loaded masses of the vehicle.;
 α – angle of rotation of the not spring-loaded mass relative to the centre of the masses of the vehicle.

Unevenness of the road or the microprofile of the road q can be viewed as a function of an array of variables with appropriately small step.

For the purpose of these calculations, assumed Voitenko [10]:

$c_1 = 320000$ N·m⁻¹ – toughness coefficient of the front tires;

$k_1 = 30000$ Ns·m⁻¹ – deformation coefficient of the front tires;

$c_2 = 320000 \text{ N}\cdot\text{m}^{-1}$ – toughness coefficient of the rear tires
 $k_2 = 30000 \text{ Ns}\cdot\text{m}^{-1}$ – deformation coefficient of the rear tires;
 $c_3 = 97240 \text{ N}\cdot\text{m}^{-1}$ – toughness coefficient of the front suspension
 $k_3 = 2200 \text{ Ns}\cdot\text{m}^{-1}$ – deformation coefficient of the front suspension;
 $c_4 = 97240 \text{ N}\cdot\text{m}^{-1}$ – toughness coefficient of the rear suspension;
 $k_4 = 2200 \text{ Ns}\cdot\text{m}^{-1}$ – deformation coefficient of the rear suspension;
 $m_1 = 130 \text{ kg}$ – not spring-loaded mass of the front axle of the vehicle;
 $m_2 = 130 \text{ kg}$ – not spring-loaded mass of the rear axle of the vehicle;
 $m = 2080 \text{ kg}$ – spring loaded mass of the vehicle (including mass m_5 in the cargo compartment);
 $I_a = 1125 \text{ kg}\cdot\text{m}^2$ – momentum of inertia of the not spring loaded mass relative to the transverse axis of the car passing through the centre of its mass.

From the results of the research (Rotenberg, 1972)

- For the front wheels:

$$q_1 = q_0(1 - \cos \omega t);$$

- For the rear wheels; as they will step into the same pit as the front wheels did after the length $(l_1 + l_2)$ at travel speed $V \text{ (m}\cdot\text{s}^{-1})$ or $V_h \text{ (km}\cdot\text{h}^{-1})$:

$$q_2 = q_0 \left[1 - \cos \omega \left(t - \frac{l_1 + l_2}{V} \right) \right];$$

$$\omega = \frac{2\pi V}{s} = \frac{2\pi V_h}{3.6s}$$

where ω – frequency of initiating influence while driving into the unevenness on the surface of the road, s^{-1} ;

s – length of the recurrence of the unevenness, m:

for asphalt surface = 0.025 m;

for paved road = 0.150 m;

for gravel surface = 0.020 m;

q_0 – offset of the depth of the unevenness from its average value, equal to the RMS value, m

for asphalt surface = 0.050 m;

for paved road = 0.015 m;

for gravel surface = 0.010 m.

If the cargo compartment has no flexible fixation points, then the differential equations of oscillations (movement) (1) ... (4) can be expressed as:

$$\ddot{z}_1 = -\frac{c_1}{m_1} \cdot (z_1 - q_1) + \frac{c_3}{m_1} \cdot (z - l_1 \cdot \alpha - z_1) - \frac{k_1}{m_1} \cdot (\dot{z}_1 - \dot{q}_1) + \frac{k_3}{m_1} \cdot (\dot{z} - l_1 \cdot \dot{\alpha} - \dot{z}_1), \quad (6)$$

$$\ddot{z}_2 = -\frac{c_2}{m_2} \cdot (z_2 - q_2) + \frac{c_4}{m_2} \cdot (z + l_2 \cdot \alpha - z_2) - \frac{k_2}{m_2} \cdot (\dot{z}_2 - \dot{q}_2) + \frac{k_4}{m_2} \cdot (\dot{z} + l_2 \cdot \dot{\alpha} - \dot{z}_2), \quad (7)$$

$$\ddot{z} = -\frac{c_3}{m} \cdot (z - l_1 \cdot \alpha - z_1) - \frac{c_4}{m} \cdot (z + l_2 \cdot \alpha - z_2) - \frac{k_3}{m} \cdot (\dot{z} - l_1 \cdot \dot{\alpha} - \dot{z}_1) - \frac{k_4}{m} \cdot (\dot{z} + l_2 \cdot \dot{\alpha} - \dot{z}_2), \quad (8)$$

$$\ddot{\alpha} = +\frac{c_3 \cdot l_1}{I_a} \cdot (z - l_1 \cdot \alpha - z_1) - \frac{c_4 \cdot l_2}{I_a} \cdot (z + l_2 \cdot \alpha - z_2) + \frac{k_3 \cdot l_1}{I_a} \cdot (\dot{z} - l_1 \cdot \dot{\alpha} - \dot{z}_1) - \frac{k_4 \cdot l_2}{I_a} \cdot (\dot{z} + l_2 \cdot \dot{\alpha} - \dot{z}_2), \quad (9)$$

And thus, the vibrations of the baggage m_5 in the luggage compartment can be expressed as:

$$z_5 = z + l_3 \cdot \alpha. \quad (10)$$

Fig. 14 and Fig. 15 show the timesweep of vibration amplitude on the centre of the mass of the chassis while traveling on paced road at $10 \text{ km}\cdot\text{h}^{-1}$ and at $60 \text{ km}\cdot\text{h}^{-1}$. When comparing data from the

images of the timesweep with the mathematically acquired data, it can be deduced that the data acquired from the mathematical model of the vehicle corresponds to the experimental data in sufficient level.

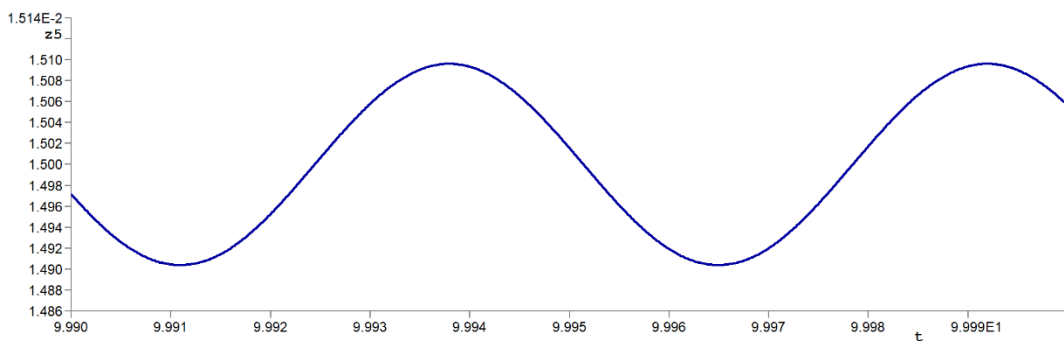


Fig. 14. Timesweep of vibration amplitude on paved road traveling at $10 \text{ km}\cdot\text{h}^{-1}$

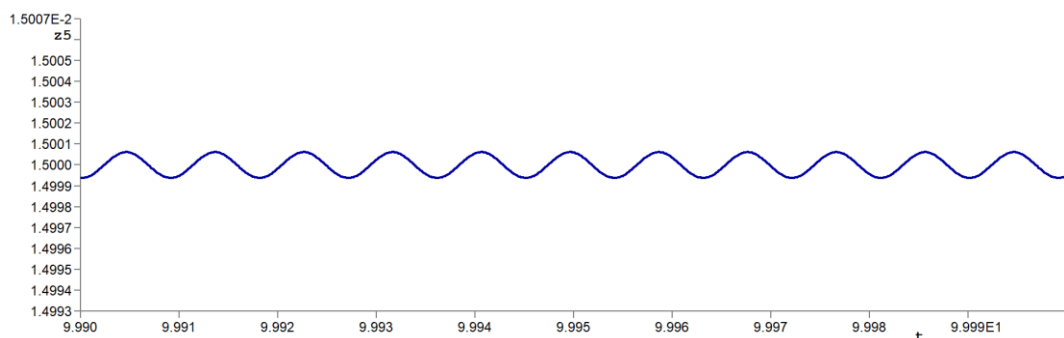


Fig. 15. Timesweep of vibration amplitude on paved road traveling at $60 \text{ km}\cdot\text{h}^{-1}$

This shows that a vehicle traveling on a paved road would have vibrations induced in it by the road; also, the faster the vehicle travels, the higher the frequency of these vibrations, while the amplitude values of the vibrations will decrease the higher the travel speed.

The same tendencies hold true when traveling on gravel and asphalt roads as well.

Conclusions

In the course of the research, test levels of vibration signals were determined on roads with various surface types at set various travel speeds. The test results show that with a vehicle travel speed increase on any of the types of road surface, the vibroacceleration of the vehicle body at the sensor installation point would also increase. The range of this increase is even exceeding 2.5 times.

The highest value of vibroacceleration at any set vehicle travel speed setting was recorded on the cobbled pavement road surface.

The acquired results of vibration levels through practical experimentation (gathered from the sensor in the cargo compartment of the vehicle) coincide with those acquired through the use of the mathematical model at accuracy level sufficient to be used in further similar vibration level studies.

The experimentally acquired data will be further useful for work on various practical tasks, for example, comparison purposes when working on further increasing precision of the mathematical models.

The experimental data will also help in creating lifelike imitation of conditions pertaining to actual road on a vibration stand in laboratory environment to further increase efficiency of performing more advanced tasks and research in the future.

Acknowledgements

This research was financed by the Aeronautics Institute of the Riga Technical University project “Prototype development of transportable in intermodal traffic mobile space testing facility “Metamorphosis”” (Metamorphosis, project No. 1.1.1.1/18/A/133) budget.

Author contributions

Investigation, D.B; methodology, D.B. and G.S. and I.S.; editing and data curation, M.H; writing—original draft preparation, M.B.; validation, L.V. All authors have read and agreed to the published version of the manuscript.

References

- [1] Бабицкий В.И. Теория виброударных систем (Theory of vibroimpact systems/V.I. Babitsky/) – М.: Наука, 1978. (In Russian)
- [2] Essien S.K. Association between whole body vibration and low back disorders in farmers: a systematic review and a prospective cohort study. A (Thesis Submitted to the College of Graduate Studies and Research In partial Fulfillment of the Requirements for the Degree of Master’s of Science) University of Saskatchewan, 2015.
- [3] Бендат, Дж., Пирсол, А. Измерение и анализ случайных процессов (Measurement and analysis of random processes). М.: Мир, 1971. (In Russian)
- [4] Griffin M. Handbook of Human Vibration/Elsevier Science, 1996.
- [5] Szczepaniak J., Tanaś W., Kromulski J. Vibration energy absorption in the whole-body system of a tractor operator. *Annals of Agricultural and Environmental Medicine*, 21(2), 2014, pp. 399-402.
- [6] Zhen Z., Griffin M. J. Response of the seated human body to whole-body vertical vibration: biodynamic responses to mechanical shocks. *Ergonomics*, 60(3). 2017, pp. 333-346
- [7] Шаняевский А.А., Банов М.Д., Беклемишев Н.Н. Диагностика усталости авиационных конструкций акустической эмиссией (Fatigue Diagnostics of Aircraft Structures by Acoustic Emission). М.: МАИ, 2017. (In Russian)
- [8] Гришкевич А.И. Автомобили: Теория: Учебник для вузов (Cars: Theory: Textbook for universities). – Мн.: Высшая школа, 1986. (In Russian)
- [9] Strautmanis G., Filimonikhin G., Gorbenko A., Strautmane V., Sansyzbajeva Z. Modelling of Transient and Steady-State Modes of a Vertical Rotor with an Automatic Balancing Device. *Journal of Vibroengineering*, 23(3), 2021, pp. 759-769. DOI: 10.21595/jve.2021.21804
- [10] Войтенко В.А. Математическое моделирование упругой подвески автомобиля. Электротехнические и компьютерные системы (Mathematical modeling of the elastic suspension of a car. Electrical and computer systems). К.: Техника, 10(86), 2013, pp. 33-40.